



Queensland University of Technology
Brisbane Australia

This is the author's version of a work that was submitted/accepted for publication in the following source:

[Zeke, Andrew J.](#), Kremers, Jan, & [Feigl, Beatrix](#) (2012) Mesopic rod and S-cone interactions revealed by modulation thresholds. *Journal of the Optical Society of America A : Optics, Image Science & Vision*, 29(2), A19-A26.

This file was downloaded from: <http://eprints.qut.edu.au/54740/>

© Copyright 2012 Optical Society of America

This paper was published in Journal of the Optical Society of America A: Optics, Image Science & Vision and is made available as an electronic reprint with the permission of OSA. The paper can be found at the following URL on the OSA website: <http://www.opticsinfobase.org/josaa/abstract.cfm?uri=josaa-29-2-A19>. Systematic or multiple reproduction or distribution to multiple locations via electronic or other means is prohibited and is subject to penalties under law.

Notice: *Changes introduced as a result of publishing processes such as copy-editing and formatting may not be reflected in this document. For a definitive version of this work, please refer to the published source:*

<http://dx.doi.org/10.1364/JOSAA.29.000A19>

Mesopic Rod and S-cone interactions revealed by modulation thresholds

Andrew J. Zele PhD^{1*}, Jan Kremers PhD², Beatrix Feigl MD PhD^{3,4}

¹ *Visual Science Laboratory, School of Optometry and Vision Science & Institute of Health and Biomedical Innovation, Queensland University of Technology, Brisbane, Australia*

² *Laboratory for Retinal Physiology, Department of Ophthalmology, University of Erlangen-Nuremberg, Erlangen Germany*

³ *Medical Retina Laboratory, Institute of Health and Biomedical Innovation, Queensland University of Technology, Brisbane, Australia*

⁴ *Queensland Eye Institute, Brisbane, Australia*

* Corresponding author: andrew.zele@qut.edu.au

Acknowledgements: Supported by the Australian Research Council ARC-DP1096354 (AJZ), a VC Research Fellowship (BF) and a QUT IHBI Visiting Researcher Fellowship (JK). We thank Aaron A'brook for technical assistance in software development and Michelle Maynard for participating in data collection.

Keywords: mesopic, temporal, rod, s-cone, summation, color

Abstract

We analyzed mesopic rod and S-cone interactions in terms of their contributions to the blue-yellow opponent pathway. Stimuli were generated using a 4-primary colorimeter. Mixed rod and S-cone modulation thresholds (constant L-, M-cone excitation) were measured as a function of their phase difference. Modulation amplitude was equated using threshold units and contrast ratios. This study identified three interaction types: (1) A linear and antagonistic rod:S-cone interaction, (2) probability summation (3) and a previously unidentified mutual nonlinear reinforcement. Linear rod:S-cone interactions occur within the blue-yellow opponent pathway. Probability summation involves signaling by different post-receptoral pathways. The origin of the nonlinear reinforcement is possibly at the photoreceptors.

1. INTRODUCTION

Vision under mesopic light levels is mediated by rod and cone photoreceptors. Anatomical and single-cell electrophysiological studies demonstrate that multiplexing of rod and cone signals in retinal ganglion cells [1] provides a neurophysiological basis for rod-cone interactions. Under mesopic light levels, physiological recordings have measured rod inputs to small bistratified ganglion cells (SBC's) of the koniocellular (KC) pathway in the retina [2, 3] and lateral geniculate nucleus [4] of the macaque, although other studies have detected little or no rod input in the retina of macaque [5] or the lateral geniculate nucleus of rhesus [6]. In comparison, physiological recordings have reliably measured rod signals in parasol ganglion cells of the magnocellular (MC) pathway in macaque [4, 5, 7], cat [8] and rhesus [6], but measurements of rod inputs to midget ganglion cells of the parvocellular (PC) pathway have been weak and variable in macaques [4, 5, 9, 10] and marmosets [11]. This study focuses on rod-cone interactions mediated via the inferred blue-yellow color opponent pathway of which the cone opponent responses of SBC's in the KC pathway are a suitable substrate [12-14]. In primates, SBC's receive ON-excitation from S-cones via S-cone (blue) ON-bipolar cells, inhibitory (OFF) input from L- and M-cones via diffuse bipolar cells [15] and have low-pass spatio-temporal characteristics to chromatic stimuli [16]. Horizontal cell feedback to the S-cone synapse creates chromatic opponency [17]. Rod inputs to SBCs have the same ON type polarity response as the S-cone under mesopic illuminations [2, 3] and mix with the inhibitory L+M signal [3]. In humans, the precise form of the interaction between rod and S-cone mediated signals is still to be determined.

Psychophysical studies have established that rod signals input to the three major afferent retinal pathways in human trichromats, namely the inferred MC, PC and KC pathways [18-20]. Interactions between rod and cone signals affect visual detection [21, 22], discrimination

[20, 23], color vision [18, 19, 24], hue perception [25-29], spatial vision [30] and temporal vision [31-35]. Rod and S-cone signal interaction has been inferred from studies using pulsed stimuli, and often in the context of understanding rod contributions to a “blue” hue percept [19, 24, 25, 36, 37]. It has been proposed that the Purkinje shift [38], the change in peak visual sensitivity from long to short wavelengths with increasing dark adaptation, involves a facilitatory interaction between rods and S-cones in normal trichromats [39] and the interaction is similarly absent in tritanopes [40, 41]. The presence of rod-cone interaction means that mesopic spectral sensitivity is not simply a linear addition of rod (V'_{λ}) and cone (V_{λ}) spectral sensitivity [42]. In S-cone monochromacy, the results are conflicting, with evidence for linear summation of rod and S-cone inputs to mesopic spectral sensitivity [43, 44] and complete independence of the rod and S-cone signals [45]. In summation studies of pulsed lights, it has been inferred for inhibition [27], near-complete additivity [46] and partial additivity [21] between rod and S-cone signals.

The temporal response of rods and cones [47], MC and PC units [48] and PC and KC units [49] differ in macaques, hence the nature of rod and S-cone interactions may differ from rod interactions with L- and M-cones. In humans, summation between photoreceptors classes has been studied using pulsed stimuli [50] and by varying the phase difference and/or amplitude of sinusoidal modulation [51]. The latter approach does not depend on knowing the temporal impulse response functions of the rod and cone pathways, which can vary due to rod-cone interaction [34]. The nature of the summation of rod and L- (or M-) cone mediated signals depends on the post-receptoral pathways mediating detection [32, 33]. Linear summation can occur when rod and L- (or M-) cone mediated signals are mediated via the same pathway. Probability summation occurs when rod and L- (or M-) cone signals are mediated via independent pathways [33]. The summation characteristics of rods and S-cones have not been

systematically studied under conditions that allow controlled examination of the phase relationship between the two-photoreceptor types when they have known signal strength.

The aim of this study is to analyze interactions between rod and S-cone modulations in terms of their underlying contributions to the blue-yellow opponent pathway in humans using a 4-primary colorimeter that independently controls rod and cone excitations. With this approach we can determine how rod and S-cone signals combine in the post-receptoral pathways mediating flicker detection.

2. METHODS

A. Apparatus and calibration procedures

A 2-channel, 4-primary Maxwellian view photostimulator [52] provided independent control of the stimulations of the rods and three types of cones in the human retina. Shapiro, Pokorny and Smith [53] describe the principles of a 4-primary colorimetric system. The primaries are derived from light-emitting diode (LED)-interference filter combinations yielding dominant wavelengths of 459 nm (blue), 516 nm (green), 561 nm (greenish yellow) and 658 nm (red). The radiances of the primaries are controlled by amplitude modulation of a 20 kHz carrier feeding into an eight-channel analog output Dolby sound card (M-Audio-Revolution 7.1 PCI) with a 24-bit digital-to-analog converter (DAC) operating at a sampling rate of 192 kHz. The output of each DAC is demodulated [54] and sent to a voltage to frequency converter that provides 1- μ s pulses at frequencies up to 250 kHz to control the LEDs [55]. The sound card with demodulator has a precision of greater than 16 bits [54]. Stimuli were generated using custom engineered software driven by a Macintosh G5 PowerPC computer.

Individual differences in prereceptoral filtering and receptoral spectral sensitivities between the observer and the CIE 1964 10° standard observer were compensated for by using observer calibration procedures conducted at the same peripheral retinal location of the stimulus field (7.5° eccentricity) as for the experiments. This method assumes an individual observer's spectral sensitivities at the primary wavelengths do not vary significantly from linear transforms of the standard observer color matching functions, as has been demonstrated [22, 52]. The observer calibration requires a photopic color match between two successively presented primary combinations (459 and 561 nm matched to 516 and 658 nm) by adjusting the luminance of the 459 nm primary, the luminance ratio of the 516 and 658 nm primaries and the combined luminance of the 516 and 658 nm primaries; the 561 nm primary is the reference light. The difference in sensitivity between the participant and the 10° standard observer was determined by comparing the relative radiances of the four primaries of the participant at the color match with the theoretical values required by the 10° standard observer [52]. The observer calibration was confirmed by two independent observations; (1) a rod pulse (500 ms, 30% contrast) that was highly conspicuous after dark adaptation was invisible after photopigment bleach and (2), the test color appearance of a rod pedestal (1 Hz, 20% contrast) when matched to a pedestal in which the cone excitations were adjusted was blue-greenish and brighter (i.e. cone excitations equivalent to a decrease in $L/[L+M]$, increase in $S/[L+M]$ and an increase in $[L+M]$) [18-20]. The physical light calibrations, observer calibration procedures and examples of the implementation of the photostimulator are described in detail elsewhere [19, 33, 34, 52, 56].

B. Psychophysical paradigms

The test stimulus was presented in a 2° circular field set in a 13° surround. A fixation point located the center of the 2° field at 7.5° eccentricity in the temporal retina. The test stimulus

was 3 cycles of a 2 Hz sinusoidal modulation above and below the time average luminance (20 Td). The measurements were performed at 2 Hz because S-cone thresholds were unmeasurable at 10 Hz within the contrast gamut of the instrument (a 10 Hz stimulus was used in studies of rod and L-cone interactions [32, 33]). The cone chromaticities at the time average retinal illuminance (20 Td) were metameric to the equal-energy-spectrum light [$L/(L+M) = 0.667$, $S/(L+M) = 1.0$] in a relative cone Troland chromaticity space [57]. We studied local (i.e. within the stimulus area) interactions using an equiluminant center and surround configuration (the time average retinal illuminance and chromaticity of the center and surround were equal) to control the adaptation across a retinal area beyond the central stimulus field.

Five photoreceptor modulation combinations were studied during which the excitation of the unmodulated classes remained constant: Rod only (constant L-, M-, S-cone excitation), S-cone only (constant rod, L- and M-cone excitation), L-cone only (constant rod, S- and M-cone excitation), mixed rod and S-cone (constant L- and M-cone excitation), and mixed rod and L-cone (constant M- and S-cone excitation). The L-cone conditions were used in the control experiment.

We used two psychophysical paradigms (Figure 1). Experiment 1 implemented a phase paradigm in which thresholds for mixed sinusoidal (2 Hz, 3 cycles) rod and S-cone modulations (constant L-, M-cone excitation) were measured as a function of their relative phase difference. Modulation amplitude was equated in threshold units (1:1TU). Experiment 2 measured thresholds for mixed rod and S-cone modulations (constant L-, M-cone excitation) as a function of the Michelson contrast ratio (0.5:1, 1:1, 2:1) of the mixed

sinusoidal modulation for two fixed phase offsets (0° and 180°) determined based on the outcomes of Experiment 1.

A control experiment confirmed that mixed rod and L-cone thresholds (1:1 TU; 2 Hz, constant M- and S-cone excitation), measured as a function of their relative phase difference (0° to 360° in 30° steps), show probability summation between independent pathways, thereby replicating a major finding of Sun et al. [33].

C. Modeling

The interaction between photoreceptor signals in post-receptoral pathways can be inferred from studies of threshold summation and symmetry of mixed stimuli (c.f. composite or compound stimuli) when shown in summation plots for the mixed stimulus as a function of the threshold for one stimulus only [58]. Data in the phase paradigm (Experiment 1) and the contrast ratio paradigm (Experiment 2) showing linear summation were modeled using vector summation, as has been used for analysis of physiological recordings of interactions in retinal ganglion cells of macaques [9, 59] and the lateral geniculate nucleus of marmosets [11], the human electroretinogram [60] and human psychophysical studies of rod-cone interaction [32, 33, 51]. In this model, the response, R , to the mixed rod and S-cone modulation is

$$R = \frac{1}{\sqrt{(r^2 + s^2 - 2 \cdot r \cdot s \cdot \cos(\phi - \phi_{r-s}))}} \quad (\text{Eq. 1})$$

and r and s represent the rod and S-cone contrast responses, ϕ is the stimulus phase (variable in the phase paradigm; 0° or 180° in the contrast ratio paradigm) and ϕ_{r-s} is the phase difference between the rod and S-cone signals. In our implementation of this model, vector summation supposes that rod and S-cone signals follow complete linear summation within

the same pathway if the mixed modulation thresholds vary as a function of the phase between the rod and S-cone modulations. The phase relationships can vary from mixed modulation thresholds being minimal when measured in-phase and maximal when measured in counter-phase, to antagonism when mixed thresholds are maximal for in-phase modulation and minimal for the counter-phase modulation, and all other outcomes fall somewhere in between. The time delay between the rod and S-cone signals can be estimated from the phase difference. The model was fit to the data by varying the parameter values to minimize the sum of squares differences using the solver routine in Excel.

Data in the phase paradigm showing probability summation were modeled using a straight line parallel to the abscissa ($R = c$) with a free vertical scaling factor (c)[33]. Figure 2 shows the model predictions for the phase paradigm. We tested the hypothesis that linear summation would be observed if rods and S-cones shared the same post-receptoral pathway and probability summation would be observed if the rod and S-cone signals were mediated via independent pathways to the detection site.

In a contrast ratio paradigm, threshold data are often described by the formula $1 = x^k + y^k$ where x and y are the components and k is the summation index [58]. If the photoreceptor signaling is completely independent, k is infinite. If the signals show complete additivity ($k = 1.0$; scalar summation), the threshold relationships have a slope of -1 in a summation plot. Supra-additivity ($k < 1.0$) occurs when the thresholds to the combined stimuli are smaller than those expected on the basis of scalar additivity (i.e. the thresholds lie between the additivity line and the axes). Partial additivity or sub-additivity of photoreceptor signals ($k > 1.0$) is observed when mixed thresholds fall between independence and complete additivity. Sub-additive data have been described theoretically in forms including inhibition, either

within [61-63] or between [64] post-receptoral pathways, by probability summation between independent pathways [58] and vector addition of orthogonal threshold mechanisms ($k = 2$)[63, 65]. The summation template $1 = x^k + y^k$ describes interactions in only one quadrant, which is adequate for pulsed stimuli [21, 62, 66, 67], and it normalizes thresholds to those for selective stimulation. It doesn't account for stimuli in which the relative phase can be varied, such as the sinusoidal modulations used in our experiments. The model is adequate for data in Experiment 2 only when the rods and S-cones were modulated with the same relative phase (either in-phase or counter-phase, but not the complete set of data). Observe that in Experiment 2 a vector summation of orthogonal mechanisms ($\phi_{r-s} = 90^\circ$) is equivalent to the summation template $1 = x^k + y^k$ with $k = 2$. For the contrast ratio experiment, our *a priori* expectation is that asymmetric contrast responses for in-phase and counter-phase conditions will be observed if mixed modulation thresholds vary as a function of the phase. In that case we expect a phase dependency in Experiment 1. In the reversed case, if in Experiment 1 thresholds are independent of phase (probability summation) then the thresholds in Experiment 2 to in-phase and counter-phase with equal contrast ratios should be the same.

D. Procedure

Observers binocularly dark-adapted for 30 min prior to the beginning of data collection. Participants used their right eye for all measurements. A chin rest maintained head position and refractive correction was inserted on the instrument side of the 2 mm artificial pupil for observer JK (-2.0 Diopters). Thresholds were measured separately for rods and S-cones. The average threshold value was used to equate the mixed rod and S-cone stimulus in 1:1 threshold units (Experiment 1). Experiments 1, 2 and the control experiment were conducted during separate sessions on separate days. One condition (stimulus phase, contrast ratio) was measured during a session. The order of conditions was randomized. A minimum of three

repeats was conducted for each condition. Data were analyzed on completion of each experiment. The rod, S-cone and L-cone thresholds were re-measured during subsequent sessions to check there were no significant changes in the threshold.

Stimulus contrast was specified according to a two-yes-one-no double random alternating staircase procedure. Observers reported their response using a button press on a hand-held gamepad. The starting contrasts of the staircases were offset by between 0.05 and 0.1 log units. The staircase controlled stimulus contrast and ended following 10 reversals at the criterion step size. The last six reversals were averaged as the measured threshold for the session. The yes/no paradigms included 10% blank trials and all observers made less than 5% false positive responses.

E. Observers

Three experienced psychophysical observers participated: the authors AJZ and JK, and a third participant (MLM) naïve to the purpose of the study. All observers have normal color vision (assessed by the Neitz OT anomaloscope) and hue discrimination (assessed by the Farnsworth-Munsell 100-Hue test). The Queensland University of Technology Human Research Ethics Committee (#0700000169) approved the experimental procedures and participants provided informed consent.

3. RESULTS

Experiment 1 (Phase paradigm)

The initial measurements included determination of the rod and S-cone threshold contrasts (Table 1). The rod thresholds are similar between observers and within the range reported

previously for comparable experimental conditions [33, 68]. The rod:S-cone threshold ratio was highest for observer MLM, indicating that rod and S-cone thresholds were similar, and lowest for observers AJZ and JK, indicating that rod and S-cone thresholds were different. The combined modulation of rod and S-cone signals is expected to reveal interaction between the post-receptoral pathways processing the photoreceptor signals. In the first experiment, thresholds were measured as a function of the phase difference between the sinusoidal rod and S-cone modulation in a 1:1 threshold ratio (constant L-, M-cone excitation). Figure 3 shows the threshold ratio (Rod + S-cone / S-cone) for the three observers as a function of the phase difference between the rod and S-cone signals (Rod = 0°). For two observers (AJZ, diamond symbols; JK, square symbols), the threshold ratio is dependent on phase, being highest for rod- and S-cone signals modulated in-phase and the lowest for counter-phase modulation. This counter-phase relationship implies an antagonistic interaction. The threshold ratio data of the third observer (MLM, circular symbols) was similar at all phase differences.

We determined whether the data could be best described by linear summation or probability summation by using one-way repeated-measures ANOVA to evaluate the null hypothesis that probability summation could explain the data. The F-ratio was significant for observers AJZ ($F_{1,4} = 26.642$, $p < 0.01$) and JK ($F_{1,4} = 59.427$, $p < 0.01$), rejecting the probability summation model and a linear summation model was fit to the data. The phase difference between rods and S-cones was estimated with the vector summation model (Eq. 1) and was 29.2° (AJZ) and 28.9° (JK) (Table 1). This means that for a maximal threshold the rod stimulus has to lead the S-cone stimulus by about 30°. For the third observer (MLM), the F-ratio was not significant ($F_{1,4} = 1.925$, $p = 0.145$), indicating threshold was independent of stimulus phase and a probability summation model ($c = 0.76$) best described the data.

Experiment 2 (Contrast ratio paradigm)

In the second experiment, we evaluated thresholds for mixed rod and S-cone modulations as a function of the contrast ratio (0.5:1, 1:1, 2:1, rod alone, S-cone alone) for two fixed phase offsets (0° and 180°). The threshold data are shown in Figure 4. The thresholds lie on straight lines through the origin. The slopes of these lines indicate the contrast ratio (grey dashed lines; labeled with R:S contrast ratio). Threshold S-cone contrast is given on the horizontal axis. Threshold rod contrast is given by the vertical axis. Data points on the abscissa indicate the threshold for an S-cone only modulation. Data points on the ordinate indicate the threshold for rod only modulation. The thresholds for the in-phase condition are displayed in the first quadrant (upper right in Figure 4). In the fourth quadrant, the thresholds for the counter-phase conditions are given (lower right in Figure 4). Only the first and fourth quadrants are shown since the second and third quadrants would show the same data because the stimuli are identical. The vector summation model predicts that the results in the two quadrants (in-phase and counter-phase conditions) can be different, whereas a probability summation model predicts that the thresholds in the two quadrants will be similar.

For the two observers who showed linear summation in the phase paradigm (AJZ, diamond symbols; JK, square symbols), thresholds for the in-phase condition decreased when the rod:S-cone contrast ratio increased from 0.5:1 to 2:1 (counter-clockwise direction). The same threshold dependency upon contrast ratio is found in the counter-phase condition in a counter-clockwise direction. That the thresholds in the two quadrants are asymmetric, with lower thresholds for the counter-phase modulation, indicates the presence of a non-linear, supra-additivity ($k < 1$) that cannot be fully explained by any of the models given in Section C. For observer MLM (circular symbols), who showed probability summation in the phase

paradigm, thresholds also decreased with increasing rod:S-cone contrast ratio but they were symmetric in the two quadrants. Thus, the thresholds were similar in the in-phase and the counter-phase conditions. That the mixed thresholds were lower for the in-phase and counter-phase modulations when compared to the stimulus alone thresholds for all observers indicates the presence of a mutual reinforcement that acts to decrease threshold when the relative strength of the rod and S-cone contrast ratio is increased. The data in Figure 4 also show that that the reinforcement of S-cone and rod signals is stronger for observer JK (square symbols) than AJZ (diamond symbols). This observation is in agreement with the data of the phase paradigm (Figure 3) and may contribute to JK having lower thresholds than AJZ.

4. DISCUSSION

This study analyzed the interactions between rod and S-cone modulations using stimulus conditions under mesopic illumination for which we can infer the post-receptoral pathway mediating detection. The summation paradigms identified three interaction types. In the phase paradigm, a linear rod:S-cone interaction is identified in observers in which the threshold contrasts to selective rod and S-cone stimulation were different (Table 1). In the observer with similar thresholds for selective rod and S-cone stimulation the phase paradigm identified probability summation. A third interaction is revealed in the contrast ratio experiment; when the relative strength of the rod and S-cone contrast ratio is increased, mutual non-linear reinforcement is found and thresholds are minimal when rods are modulated with twice the contrast of the S-cones (2:1).

We tested the hypothesis that linear interaction in the phase paradigm would be detected if the rods and S-cones shared the same post-receptoral pathway (Figure 2, 3). The data in the phase paradigm support this hypothesis and indicate that mixed rod and S-cone modulation

thresholds are phase dependent, being lowest when modulated in approximate counter-phase, indicating the presence of an antagonistic interaction. We infer that the linear rod:S-cone interactions in two observers occur at a common locus, possibly within the blue-yellow color opponent pathway, of which the small bistratified cells are a likely substrate. Our finding for linear summation differs from past studies wherein summation ranged from partial to near-complete summation [21, 27, 46]. Methodological differences between studies will affect the relative rod and S-cone photoreceptor sensitivities and their temporal responses; this study measured rod and S-cone summation with photoreceptor-class specific sinusoidal modulation whereas previous studies used pulsed stimuli of different wavelengths. The finding for linear summation of rod:S-cone signals within the inferred KC pathway is consistent with evidence from psychophysical studies for interactions between rods and S-cones in their contribution to a “blue” hue percept [19, 69]. There is also psychophysical evidence for interactions in chromatic discrimination, where rods suppress S-cone decrement discrimination [20, 70], due to interactions between the luminance (L+M) signal from rods and the chromatic signal from the S-cones [31]. In temporal processing, rods are known to also interact strongly with L+M cone signals [31, 34]. Our data indicate that linear interactions can occur but that this may be the case in only in particular circumstances. When the ratio of rod to cone modulation changes, then the characteristics of the linear interaction may also change.

Physiological recording in macaque retina and LGN show that rod signals mix with S-cone signals [2-4]. At 20 Td, the adaptation level of this study, rod input to the SBCs is likely mediated via gap junctions between photoreceptors. The inhibitory L+M response is replaced by an excitatory response with the same sign input as the S-cones [2-4], but the rod signals can also mix with the LM-OFF signals [3]. Based on the data from the two observers showing linear summation in Figure 3, thresholds were lowest when the rod modulation led

the S-cone, consistent with the rod signal being phase delayed relative to the S-cone signal. Although these data do not rule out the possibility of an additive interaction of the rod-ON signal in the excitatory field of the SBC, the antagonistic nature of the linear interaction is consistent with rod interactions with the inhibitory L+M-OFF response. In the following we consider the phase relationship between the rod and S-cone data.

The summation characteristics of rod and cone signals are consistent with temporal frequency dependent latency differences between photoreceptor classes, as demonstrated in the magnocellular pathway [5]. Physiological measurements of the temporal response of the koniocellular pathway indicate the time-to-peak of the excitatory (Blue-ON) signal is 10-20 ms shorter than the inhibitory (yellow-OFF) signal [71] and SBC dynamics decrease with decreasing illumination [2], consistent with a delay in the time-to-peak of the impulse response function for rod and cone inputs to the inferred MC pathway with decreasing illumination [72]. Psychophysically, the latency of S-opponent signals is longer than L-M opponent signals by between 20-30 ms [73] and ~40 ms [74], in the range of physiological estimates of latency differences between S-opponent and L-M opponent signals recorded in V1 of macaques [75]. Within the S-cone pathway, the S-OFF signal is delayed relative to the S-ON signal under photopic illumination, with estimates ranging between about 25 ms [76] and 50 ms [77]. At present there are no psychophysical estimates of changes in the latency of the blue-yellow opponent pathway, or of differences in rod and S-cone latencies, under mesopic illumination. Based on the data reported in this study, one could speculate that if under mesopic illumination, the rod stimuli have to be phase advanced by about 30° to the S-cone stimuli for maximal cancellation, then rod signals arrive about 40 ms later than cone signals.

For observer MLM who showed probability summation, we infer, that rod thresholds are likely to be signaled via the inferred magnocellular pathway based on the summation data of Sun et al. [33]. One difference between observers in this study was their threshold contrasts for selective rod and S-cone stimulation (Threshold ratio; Table 1). Probability summation was detected when thresholds were similar for selective rod and S-cone stimulation. These individual differences may depend on factors including the stimulus temporal frequency [68] and the relative level of rod and S-cone excitation at the adaptation level. Linear summation of S-cone signals occurs in retinal circuits when the strength of the physiological connections is linearly proportional to the number of anatomically defined synapses [71]. The generality of that observation [71] may not hold under other conditions including when rods are active, with plastic changes in the physiological strength of cortical circuits [78] and in the presence of interactions. There is evidence from common marmosets that rod to cone signal strengths also vary as a function of eccentricity in different ganglion cells types (MC, PC) [11] but this has not been replicated in macaques at the test eccentricities studied [5], nor are there equivalent measurements for the S-cone pathway. Further studies, with larger sample sizes, are required to determine if a change in test parameters (e.g. chromaticity, adaptation level, temporal frequency) can shift the rod:S-cone interaction between linear and probability summation.

The contrast ratio data confirms the predictions from the data in the phase paradigm and identified an additional and previously unknown interaction type (Figure 4). The prediction from the linear summation data is an asymmetry between the in-phase and counter-phase data in the contrast ratio paradigm and the prediction from the probability summation data is for symmetric contrast responses. This indeed was found in the three observers. However, in comparison with the phase paradigm, where rod and S-cone strength was equated in

threshold units (1:1), the relative strength of the rod and S-cone signals is altered in the contrast ratio experiment. This results in a non-linear interaction. S-cone and rod signals reinforce each other when stimulated simultaneously. Moreover the reinforcement depends on the contrast ratio and is maximal when rod:S-cone contrast ratio is about two. The nonlinear reinforcement is an indication for supra-additivity given that thresholds are smaller for simultaneous rod and S-cone modulation than is predicted on the basis of complete additivity. We would not consider this interaction as same-sign additivity because it acts in a similar manner when the two photoreceptor classes are modulated in-phase and in counter-phase. Therefore, it is indicative of a mechanism that is independent from the opposite-sign additivity found in the phase paradigm. The physiological basis of this non-linear reinforcement is unclear. The reinforcement is also present in the observer showing probability summation in the phase paradigm and thus rod and S-cone signal transmission in separate post-receptoral pathways gives no possibility for further interactions. This suggests that the nonlinear interaction should occur before the rod and S-cone signals input to the inferred koniocellular and magnocellular pathways, possibly at a photoreceptor level and may involve gap junctions between rods and cones rather than cone specific horizontal cell syncytium [79]. That the nonlinearity is present in the data of all three observers is consistent with this hypothesis.

We conclude that linear rod:S-cone interaction under mesopic light levels occurs within the blue-yellow opponent pathway when rod to S-cone contrast ratio is constant and the thresholds to rod and S-cone isolating stimuli are different. A shift to probability summation involves signaling by different pathways, with rod thresholds likely to be signaled via the inferred magnocellular pathway and may occur when thresholds for S-cone and rod isolating stimuli are similar, but additional studies are required to further understand this observation.

The contrast ratio data indicate the presence of strong non-linear interaction between rods and S-cones when the ratio between rod and S-cone contrast is varied. This non-linear interaction may be present at the photoreceptors.

5. REFERENCES

1. N. W. Daw, E. J. Jensen, and W. J. Bunkin, "Rod pathways in the mammalian retinae," *Trends Neurosci.* **13**, 110-115 (1990).
2. G. D. Field, M. Greschner, J. L. Gauthier, C. Rangel, J. Shlens, A. Sher, D. W. Marshak, A. M. Litke, and E. J. Chichilnisky, "High-sensitivity rod photoreceptor input to the blue-yellow color opponent pathway in macaque retina," *Nat. Neurosci.* **12**, 1159-1164 (2009).
3. J. D. Crook, C. M. Davenport, B. B. Peterson, O. S. Packer, P. B. Detwiler, and D. M. Dacey, "Parallel ON and OFF cone bipolar inputs establish spatially coextensive receptive field structure of blue-yellow ganglion cells in primate retina," *J. Neurosci.* **29**, 8372-8387 (2009).
4. V. Virsu and B. B. Lee, "Light adaptation in cells of macaque lateral geniculate nucleus and its relation to human light adaptation," *J. Neurophysiol.* **50**, 864-878 (1983).
5. B. B. Lee, V. C. Smith, J. Pokorny, and J. Kremers, "Rod inputs to macaque ganglion cells," *Vision Res.* **37**, 2813-2828 (1997).
6. T. Wiesel and D. H. Hubel, "Spatial and chromatic interactions in the lateral geniculate body of the rhesus monkey," *J. Neurophysiol.* **29**, 1115-1156 (1966).
7. D. Cao, B. B. Lee, and H. Sun, "Combination of rod and cone inputs in parasol ganglion cells of the magnocellular pathway," *J. Vision* **10**, 4 (2010).
8. V. Virsu, B. B. Lee, and O. D. Creutzfeldt, "Dark adaptation and receptive field organisation of cells in the cat lateral geniculate nucleus," *Exp. Br. Res.* **27**, 35-50 (1977).

9. B. B. Lee, J. Pokorny, V. C. Smith, P. R. Martin, and A. Valberg, "Luminance and chromatic modulation sensitivity of macaque ganglion cells and human observers," *J. Opt. Soc. Am. A* **7**, 2223-2236 (1990).
10. K. Purpura, D. Tranchina, E. Kaplan, and R. M. Shapley, "Light adaptation in the primate retina: analysis of changes in gain and dynamics of monkey retinal ganglion cells," *Vis. Neurosci.* **4**, 75-93 (1990).
11. S. Weiss, J. Kremers, and J. Maurer, "Interaction between rod and cone signals in responses of lateral geniculate neurons in dichromatic marmosets (*Callithrix jacchus*)," *Vis. Neurosci.* **15**, 931-943 (1998).
12. D. M. Dacey, "Morphology of a small-field bistratified ganglion cell type in the macaque and human retina," *Vis. Neurosci.* **10**, 1081-1038 (1993).
13. D. M. Dacey and B. B. Lee, "The 'blue-on' opponent pathway in primate retina originates from a distinct bistratified ganglion cell type," *Nature* **367**, 731-735 (1994).
14. G. D. Field, J. L. Gauthier, A. Sher, M. Greschner, T. A. Machado, L. H. Jepson, J. Shlens, D. E. Gunning, K. Mathieson, W. Dabrowski, L. Paninski, A. M. Litke, and E. J. Chichilnisky, "Functional connectivity in the retina at the resolution of photoreceptors," *Nature* **467**, 673-677 (2010).
15. B. B. Lee, P. R. Martin, and U. Grunert, "Retinal connectivity and primate vision," *Prog. Ret. Eye Res.* **29**, 622-639 (2010).
16. T. Yeh, B. B. Lee, and J. Kremers, "The temporal response of ganglion cells of the macaque retina to cone-specific modulation," *J. Opt. Soc. Am. A* **12**, 456-464 (1995).
17. O. S. Packer, J. Verweij, P. H. Li, J. L. Schnapf, and D. M. Dacey, "Blue-yellow opponency in primate S cone photoreceptors," *J. Neurosci.* **30**, 568-572 (2010).
18. D. Cao, J. Pokorny, and V. C. Smith, "Matching rod percepts with cone stimuli," *Vision Res.* **45**, 2119-2128 (2005).

19. D. Cao, J. Pokorny, V. C. Smith, and A. J. Zele, "Rod contributions to color perception: linear with rod contrast," *Vision Res.* **48**, 2586-2592 (2008).
20. D. Cao, A. J. Zele, and J. Pokorny, "Chromatic discrimination in the presence of incremental and decremental rod pedestals," *Vis. Neurosci.* **25**, 399-404 (2008).
21. S. L. Buck, E. Sanocki, and R. Knight, "Do rod signals add with S cone signals in increment detection," in *Colour Vision Deficiencies*, C. R. Cavonius, ed. (Kluwer, Dordrecht, 1997), pp. 451-458.
22. H. Sun, J. Pokorny, and V. C. Smith, "Brightness Induction from rods," *J. Vision* **1**, 32-41 (2001).
23. R. Knight, S. L. Buck, G. A. Fowler, and A. Nguyen, "Rods affect S-cone discrimination on the Farnsworth-Munsell 100-hue test," *Vision Res.* **38**, 3477-3481 (1998).
24. J. Pokorny, M. Lutze, D. Cao, and A. J. Zele, "The color of night: Surface color perception under dim illuminations," *Vis. Neurosci.* **23**, 525-530 (2006).
25. E. N. Willmer, "Low threshold rods and the perception of blue," *J. Physiol. (Lond)*. **111**, 17P (1949).
26. I. Lie, "Dark adaptation and the photochromatic interval," *Doc. Ophthalmol.* **17**, 411-510 (1963).
27. P. W. Trezona, "Rod participation in the 'blue' mechanism and its effect on colour matching," *Vision Res.* **10**, 317-332 (1970).
28. U. Stabell and B. Stabell, "Chromatic rod vision. II. Wavelength of pre-stimulation varied," *Scand. J. Psychol.* **12**, 282-288 (1971).
29. S. L. Buck, R. Knight, G. Fowler, and B. Hunt, "Rod influence on hue-scaling functions," *Vision Res.* **38**, 3259-3263 (1998).

30. G. Lange, N. Denny, and T. E. Frumkes, "Suppressive rod-cone interactions: evidence for separate retinal (temporal) and extraretinal (spatial) mechanisms in achromatic vision," *J. Opt. Soc. Am. A* **14**, 2487-2498 (1997).
31. D. Cao, A. J. Zele, and J. Pokorny, "Dark-adapted rod suppression of cone flicker detection: Evaluation of receptor and postreceptor interactions," *Vis. Neurosci.* **23**, 531-537 (2006).
32. J. Kremers and S. Meierkord, "Rod-cone-interactions in deuteranopic observers: models and dynamics," *Vision Res.* **39**, 3372-3385 (1999).
33. H. Sun, J. Pokorny, and V. C. Smith, "Rod-cone interaction assessed in inferred magnocellular and parvocellular postreceptor pathways," *J. Vision* **1**, 42-54 (2001).
34. A. J. Zele, D. Cao, and J. Pokorny, "Rod-cone interactions and the temporal impulse response of the cone pathway," *Vision Res.* **48**, 2593-2598 (2008).
35. A. J. Zele and A. J. Vingrys, "Defining the detection mechanisms for symmetric and rectified flicker stimuli," *Vision Res.* **47**, 2700-2713 (2007).
36. W. Nagel, "Appendix: Adaptation, Twilight Vision and the Duplicity Theory," in *Helmholtz's Treatise on Physiological Optics. Translated from the Third German Edition by J.P.C. Southall*, Third German Edition ed. (Optical Society of America, Rochester, New York, 1924), pp. 313-343.
37. S. L. Buck, "What is the hue of rod vision?," *Color Research and Application* **26**, S57-S59 (2001).
38. J. Purkinje, *Beobachtungen und Versuche zur Physiologie der Sinne. Neue Beiträge zur Kenntniss des Sehens in subjectiver Hinsicht*. (Reimer, Berlin, 1825), pp. 1-192.
39. E. A. Hough, "The spectral sensitivity functions for parafoveal vision," *Vision Res.* **8**, 1423-1430 (1968).

40. E. A. Hough and K. H. Ruddock, "The parafoveal visual response of a tritanope and an interpretation of the V lambda sensitivity functions of mesopic vision," *Vision Res.* **9**, 935-946 (1969).
41. E. A. Hough and K. H. Ruddock, "The Purkinje shift," *Vision Res.* **9**, 313-315 (1969).
42. CIE, "Mesopic photometry: History, special problems and practical solutions. Publ. CIE No.81," Bureau Central de la CIE, Paris, TC 1-01 (1989).
43. H. R. Blackwell and O. M. Blackwell, "Rod and cone receptor mechanisms in typical and atypical congenital achromatopsia," *Vision Res.* **1**, 62-107 (1961).
44. J. Pokorny, V. C. Smith, and R. Swartley, "Threshold measurements of spectral sensitivity in a blue monocone monochromat," *Invest. Ophthalmol.* **9**, 807-813 (1970).
45. M. Alpern, G. B. Lee, and B. E. Spivey, "Pi-1 Cone Monochromatism," *Arch. Ophthalmol.* **74**, 334-337 (1965).
46. F. Naarendorp, K. S. Rice, and P. A. Sieving, "Summation of rod and S cone signals at threshold in human observers," *Vision Res.* **36**, 2681-2688 (1996).
47. J. L. Schnapf, B. J. Nunn, M. Meister, and D. A. Baylor, "Visual transduction in cones of the monkey *Macaca fascicularis*," *J. Physiol. (Lond)*. **427**, 681-713 (1990).
48. V. C. Smith, J. Pokorny, B. B. Lee, and D. M. Dacey, "Sequential processing in vision: The interaction of sensitivity regulation and temporal dynamics," *Vision Res.* **48**, 2649-2656 (2008).
49. E. Kaplan, "The M, P, and K pathways of the primate visual system," in *The Visual Neurosciences*, L. M. Chalupa and J. S. Werner, eds. (MIT Press, Cambridge MA, 2004), pp. 481-493.

50. R. M. Boynton, M. Ikeda, and W. S. Stiles, "Interactions among chromatic mechanisms as inferred from positive and negative increment thresholds," *Vision Res.* **4**, 87 (1964).
51. T. J. T. P. van den Berg and H. Spekreijse, "Interaction between rod and cone signals studied with temporal sine wave stimulation," *J. Opt. Soc. Am.* **67**, 1210-1217 (1977).
52. J. Pokorny, H. Smithson, and J. Quinlan, "Photostimulator allowing independent control of rods and the three cone types," *Vis. Neurosci.* **21**, 263-267 (2004).
53. A. G. Shapiro, J. Pokorny, and V. C. Smith, "Cone-Rod receptor spaces, with illustrations that use CRT phosphor and light-emitting-diode spectra," *J. Opt. Soc. Am. A* **13**, 2319-2328 (1996).
54. M. J. Puts, J. Pokorny, J. Quinlan, and L. Glennie, "Audiophile hardware in vision science; the soundcard as a digital to analog converter," *J. Neurosci. Meth.* **142**, 77-81 (2005).
55. W. H. Swanson, T. Ueno, V. C. Smith, and J. Pokorny, "Temporal modulation sensitivity and pulse detection thresholds for chromatic and luminance perturbations," *J. Opt. Soc. Am. A* **4**, 1992-2005 (1987).
56. A. J. Zele, D. Cao, and J. Pokorny, "Threshold units: A correct metric for reaction time?," *Vision Res.* **47**, 608-611 (2007).
57. V. C. Smith and J. Pokorny, "The design and use of a cone chromaticity space," *Color Res. Appl.* **21**, 375-383 (1996).
58. N. V. S. Graham, *Visual Pattern Analyzers* (Oxford University Press, New York, 1989), pp. 1-646.
59. V. C. Smith, B. B. Lee, J. Pokorny, P. R. Martin, and A. Valberg, "Responses of macaque ganglion cells to the relative phase of heterochromatically modulated lights," *J. Physiol. (Lond)*. **458**, 191-221 (1992).

60. J. Kremers, T. Usui, H. P. Scholl, and L. T. Sharpe, "Cone signal contributions to electroretinograms in dichromats and trichromats," *Invest. Ophthalmol. Visual Sci.* **40**, 920-930 (1999).
61. N. Benimoff, S. Schneider, and D. C. Hood, "Interactions between rod and cone channels above threshold: A test of various models," *Vision Res.* **22**, 1133-1140 (1982).
62. B. Drum, "Summation of rod and cone responses at absolute threshold," *Vision Res.* **22**, 823-826, (1982).
63. S. L. Guth, N. J. Donley, and R. T. Marrocco, "On luminance additivity and related topics," *Vision Res.* **9**, 537-575 (1969).
64. M. W. Levine and L. J. Frishman, "Interactions between rod and cone channels: a model that includes inhibition," *Vision Res.* **24**, 513-516 (1984).
65. R. W. Massof and S. J. Starr, "Vector magnitude operation in color vision models: derivation from signal detection theory," *J. Opt. Soc. Am.* **70**, 870-872 (1980).
66. S. L. Buck and R. Knight, "Test-additivity experiments: different procedures, different results," *J. Opt. Soc. Am. A* **8**, 696-698 (1991).
67. S. L. Buck and R. Knight, "Partial additivity of rod signals with M- and L-cone signals in increment detection," *Vision Res.* **34**, 2537-2545 (1994).
68. H. Sun, J. Pokorny, and V. C. Smith, "Control of the modulation of human photoreceptors," *Color Res. Appl.* **26**, S69-S75 (2001).
69. S. L. Buck, "Rod-cone interactions in human vision," in *The Visual Neurosciences*, L. M. Chalupa and J. S. Werner, eds. (MIT Press, Cambridge MA, 2004), pp. 863-878.
70. R. Knight, S. L. Buck, and M. Pereverzeva, "Stimulus Size Affects Rod Influence on Tritan Chromatic Discrimination," *Color Res. Appl.* **26**, S65-S68 (2001).

71. E. J. Chichilnisky and D. A. Baylor, "Receptive-field microstructure of blue-yellow ganglion cells in primate retina," *Nat. Neurosci.* **2**, 889-893 (1999).
72. D. Cao, A. J. Zeile, and J. Pokorny, "Linking impulse response functions to reaction time: Rod and cone reaction time data and a computational model," *Vision Res.* **47**, 1060-1074 (2007).
73. H. E. Smithson and J. D. Mollon, "Is the S-opponent chromatic sub-system sluggish?," *Vision Res.* **44**, 2919-2929 (2004).
74. D. J. McKeefry, N. R. Parry, and I. J. Murray, "Simple reaction times in color space: the influence of chromaticity, contrast, and cone opponency," *Invest. Ophthalmol. Visual Sci.* **44**, 2267-2276 (2003).
75. N. P. Cottaris and R. L. De Valois, "Temporal dynamics of chromatic tuning in macaque primary visual cortex," *Nature* **395**, 896-900 (1998).
76. C. Ripamonti, W. L. Woo, E. Crowther, and A. Stockman, "The S-cone contribution to luminance depends on the M- and L-cone adaptation levels: silent surrounds?," *J. Vision* **9**, 10 11-16 (2009).
77. K. Shinomori and J. S. Werner, "The impulse response of S-cone pathways in detection of increments and decrements," *Vis. Neurosci.* **25**, 341-347 (2008).
78. P. Sterling, "Deciphering the retina's wiring diagram," *Nat. Neurosci.* **2**, 851-853 (1999).
79. D. M. Dacey, B. B. Lee, D. K. Stafford, J. Pokorny, and V. C. Smith, "Horizontal cells of the primate retina: Cone specificity without spectral opponency," *Science* **271**, 656-659 (1996).

TABLE

Table 1. Threshold contrasts and vector summation model parameters.

Observer	Threshold Contrast		Threshold Ratio	Vector Summation Model (Eq. 1)		
				Photoreceptor Signal Strength (r, s)		Phase Difference (ϕ_{r-s})
	Rod	S-cone		Rod	S-cone	
AJZ	0.084	0.178	0.47	2.69	0.92	29.2°
JK	0.081	0.223	0.36	1.49	0.61	28.9°
MLM	0.117	0.141	0.84	-	-	-

FIGURE LEGENDS

Figure 1. (Color online) Experimental paradigms. Schematic of the relative phase differences between rod (black dotted lines) and S-cone (blue dashed lines) modulations for the phase paradigm (Experiment 1: Top) and contrast ratio paradigm (Experiments 2; Bottom). In the phase paradigm, threshold ratio (1:1 Threshold Units) defines the relative amplitude of the two modulation types. In the contrast ratio paradigm, Michelson contrast ratio (0.5:1, 1:1, 2:1) defines the photoreceptor modulation amplitudes.

Figure 2. (Color online) Model predictions for the phase paradigm. In Experiment 1, the rod and S-cone modulations were maintained in a constant ratio of 1:1 threshold units as a function of the phase difference (degrees) between the photoreceptor modulations. Two outcomes were tested. For linear summation (within-pathway summation), threshold is dependent on the phase difference between the mixed photoreceptor modulations. Three predictions are shown for linear summation. The dashed line (blue) shows linear summation (phase = 30°) with a threshold ratio (TR) less than one ($TR < 1.0$; sub-additivity). The solid line (black) shows linear summation (phase = 30°) with a threshold ratio (TR) larger than one ($TR > 1.0$; supra-additivity). The dotted line (red) shows linear summation (phase = 180° ; $TR < 1.0$). In these examples, the difference between the 30° and 180° phase difference is due to antagonistic interaction. For probability summation (gray dashed-dot line; $c = 0.75$), threshold is independent of the phase difference between the mixed photoreceptor modulations.

Figure 3. (Color online) Thresholds for combined rod and S-cone modulation as a function of their relative phase difference (degrees) at 20 photopic Td with an equiluminant surround

(Experiment 1). Symbols show the data (mean \pm standard deviation) for the three observers (diamonds, AJZ; squares JK; circles, MLM). The lines show the best-fitting models (linear summation, AJZ and JK; probability summation, MLM). Error bars are smaller than some symbols.

Figure 4. (Color online) Thresholds for combined rod and S-cone modulation as a function of the Michelson contrast ratio (0.5:1, 1:1, 2:1, rod alone, S-cone alone) for two phases (0° and 180°) at 20 photopic Td with an equiluminant surround (Experiment 2). Symbols show the mean data (average standard deviation = 0.0059%) for the three observers (diamonds and solid line, AJZ; squares and dashed line JK; circles and dotted line, MLM).

Figure 1.

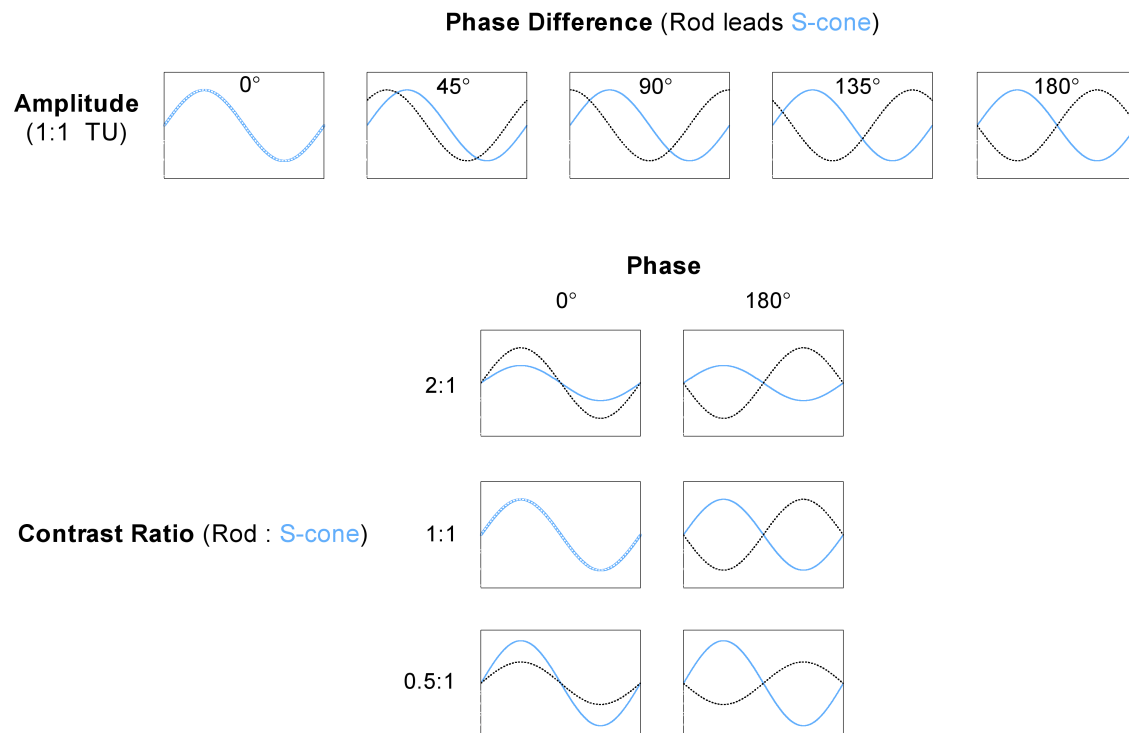


Figure 2.

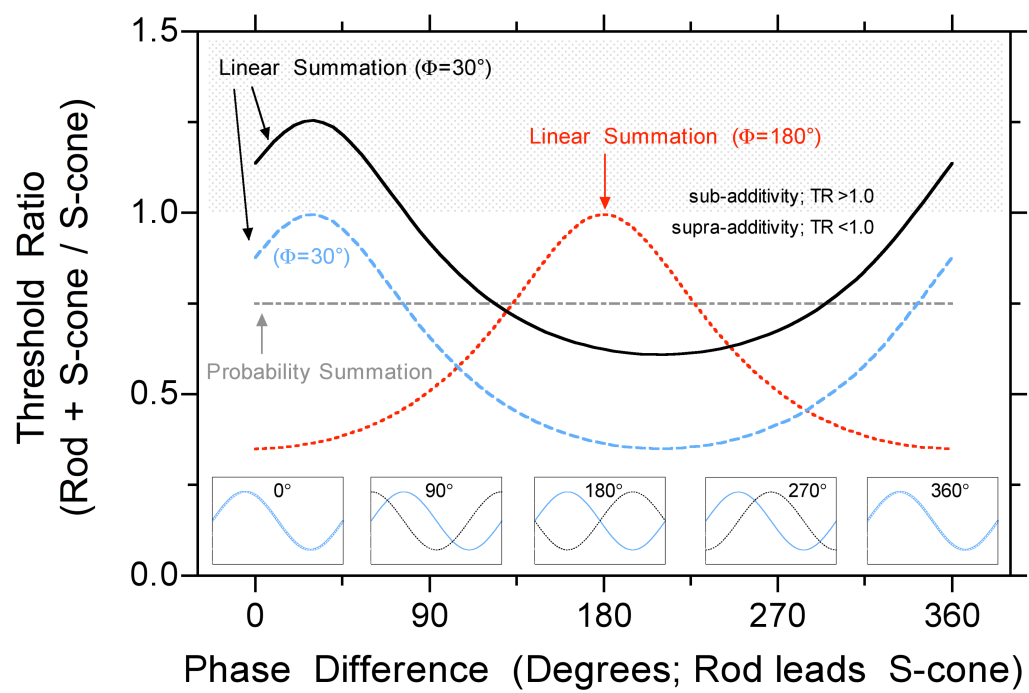


Figure 3.

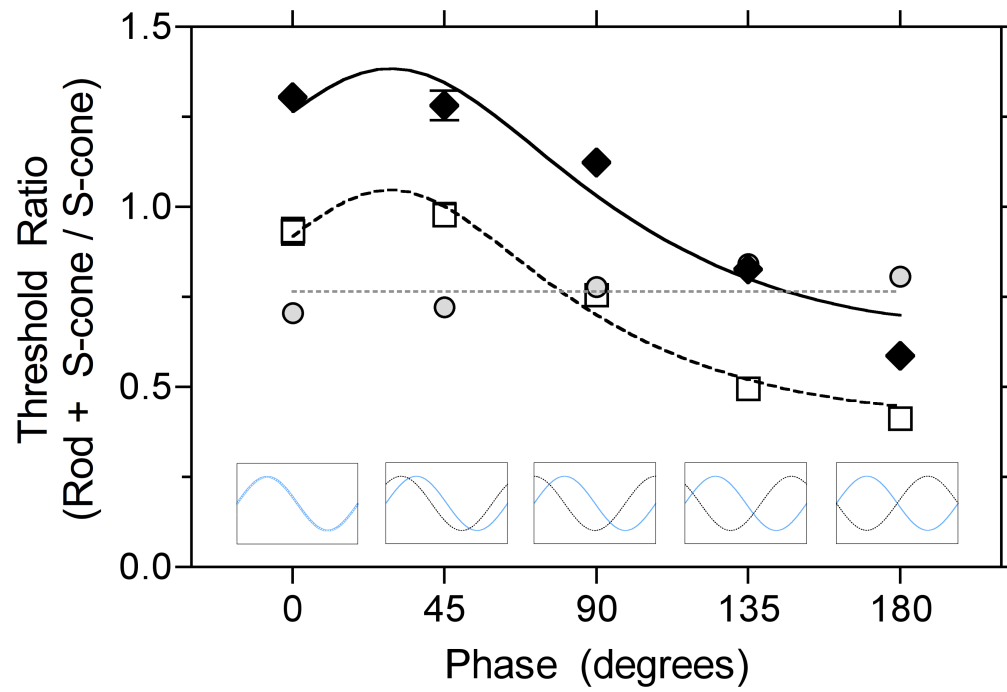


Figure 4.

